PROCEEDINGS, 44th Workshop on Geothermal Reservoir Engineering
Stanford University, Stanford, California, February 11-13, 2019
SGP-TR-214

Thermal Mapping of Icelandic Geothermal Surface Manifestations with a Drone

Grimur Bjornsson[1], Gunnar Grimsson[2], Ari Sigurdsson[3] and Valdimar S. Laenen[4]

Warm Arctic, Skjolbraut 22, IS-200 Kopavogur, Iceland

grimur.bjornsson@gmail.com[1], grimsson.gunnar@gmail.com[2], arithorlacius@gmail.com[3], steinar9@gmail.com[4]

Keywords: Drone, thermal camera, thermal maps, orthomosaics, GIS, Iceland, Geysir, Svartsengi, Eldfell, Snæfellsjökull

ABSTRACT

Rapid advances and developments in drone technologies have made mapping of geothermal surface manifestations doable and routine. In this study a DJI Matrice 210 drone, equipped with optical and thermal cameras, successfully maps some 1-4 km^2 per day. Deliverables are an orthomosaic aerial and digital surface models (DSM) and a thermal reflectance map in °C. Data gathered from relatively low altitude flights, no more than 250 meters above ground surface, yields orthomosaic resolutions of only few centimeters/pixel and thermal resolutions of 20-30 cm. The thermal imagery is manipulated to be effectively processed to a map and ran through atmospheric corrections to maximize accuracy in °C. In this paper, thermal maps collected in four Icelandic locations are shown to produce lineaments of geothermal importance simply by ignoring all temperatures below a certain threshold. With this approach N-S oriented and a few hundred-meter-long structures in Svartsengi are inferred. The 1973 Eldfell eruption on Heimaey island in S-Iceland is still emitting heat to surface, inferring the thick basaltic lave pile deposited 45 years ago is yet to be fully solidified. The Geysir hot spring area thermal map is confirming previously published N-S orientation of the field main upflow zone, complemented with new warm surface areas and vivid convection cells in the hot water bowls of Strokkur and Geysir eruptive hot springs. The east flanks of Snæfellsjökull, a glaciated stratovolcano, are suspected to be heated by a deep seated and currently hidden boiling geothermal reservoir, by cross correlating high elevation vegetation growth, gaps in the snow cover and gently warm grounds.

1. INTRODUCTION

Unmanned aerial vehicles (UAVs), or simply drones, have advanced rapidly in recent years. Drone operations are becoming fairly user-friendly and expenditure of equipment has likewise dropped significantly. This development is a welcomed fast and cost-effective geothermal exploration opportunity. Warm Arctic therefore decided to purchase its own fully integrated unit in early 2018. The acquired drone is DJI® Matrice 210, which is dual-equipped with a Zenmuse X4S high resolution optical camera and a Zenmuse XT 640x512 radiometric thermal camera from FLIR®. This is a bundled package and only introduced in summer 2017. With ample geothermal surface manifestations within 40-minute drive from Reykjavik, the capital of Iceland, experimentation and familiarization of the equipment proved fast and fruitful. Processing of the thermal imagery into maps proved to be less straightforward. With the aid of open source software, however, it was possible to extract the raw thermal values embedded in the proprietary R-JPEG format, perform atmospheric corrections, convert to temperature values and simplify the map-making process. Finally, by purchasing additional batteries and chargers, the drone has proven to be able to map over 4 km^2 of terrain per day. This requires operating both cameras simultaneously for maximum data gathering and taking advantage of long winter nights at Iceland´s northerly latitude.

In this paper the authors like to share some of the experience with the geothermal community. Following a section on previous drone thermal surveys, the Warm Arctic drone and its accessories are described. We then proceed to introduce field data from various locations in Iceland. The paper ends with way forward analysis.

2. PREVIOUS WORK

Although drone surveying is fairly mature in geothermal exploration, the addition of a thermal camera is more recent. We have in particular followed the work of M. Harwey and his New Zealand and international colleagues on drone mapping (Harwey et al, 2014; Harwey et al, 2015; Harwey et al., 2016a; Harwey et al, 2016b). Some of this work commenced prior to the introduction of ready-made and fully integrated commercial drones for thermal mapping. In this pioneering work simple drones were apparently modified to carry a thermal camera. The resulting outputs are temperature-calibrated thermal maps together with aerial maps (orthomosaics) and digital elevation models. Work focused on New Zealand geothermal fields and has generated interesting byproducts to the surface temperature such as the heat loss of a geothermal resource. Other authors from locations such as Malaysia (Abubakar et al., 2017) and Russia (Cherkasov et al., 2018) discuss the applicability of thermal remote sensing and couple with conceptual geothermal reservoir models. Vaughan et al. (2018) mapped the Casa Diablo Geothermal Field with a fixed wing aircraft flown over night at 1800 m above ground surface. This study was able to generate a large 51 km^2 thermal map but the resolution is about 1 m pixel size due to the high elevation of the thermal camera. Ólafsson (2018) analyzed recent thermal maps from the Krýsuvík area in SW-Iceland to explain the nature of large hot spring outflow and its surroundings. Finally, González (2018) also mapped thermal manifestations in the same Krýsuvík area, this time comparing drone images with satellite data to better assess heat flow from a thermal image study area of less than a hectare.

We find interesting that in most of the above work fairly small areas of thermal mapping are presented, generally they are within 3 km^2 per project except for Casa Diablo. If adopting 5-10 MW/km^2 power density in high temperature operations a more ambitious thermal mapping coverage is needed for many current or planned large geothermal power plants. The drone discussed in this paper appears ready for such large exploration work.

3. THE MATRICE 210 DRONE AND ACCESSORIES

Figure 1 is showing the Matrice 210 drone component when ready for field surveying. In our operations contingency is on multiple batteries (12 pieces of TB50 batteries, each pair good for about 20-minute flight time), two sets of rotor blades, two chargers and two tablets for the drone preprogrammed operations. The silver colored battery safe-bags are for protection and easier airport security. The quadcopter itself, remote controller and the two cameras are all single copies. A sophisticated carrying box ensures safe transport of the drone; its weight with batteries is about 30 kilos. The carrying case is accepted as checked luggage on international flights excluding batteries.

Figure 1: The Matrice 210 drone with accessories (left) and carrying case (right)

There was an initial learning curve and a handful of teething problems to overcome before the drone unit was considered ready for massive prospecting. For example, DJI’s official software updates and patches for the drone and the batteries are quite common and bothersome. A variety of drone operation software is on the market for the preprogrammed flights in a systematic grid-based method. Such software takes experience and exercising prior to flawless operations. In some instances, we have made the drone fly up to 1.8 km long flight lines in a flight grid. In that scenario it is important to minimize overlapping of flight lines from a common origin for better ratio of new images to total flight time, as it allows for near constant recharging of batteries and increasing data gathering efficiency. Bringing a small generator along with the field crew is handy. Then more than 6 serial flights are possible with the 10-12 batteries, allowing for up to 2 km^2 of coverage during early morning flights and another 1-2 km^2 near sunset. Sometimes a compromise needs to be made between covered area (battery supply) and map resolution. Flight heights over point of origin are therefore generally in the 200-250 m range and overlapping has to be substantial. Large birds of prey were recently an issue in an Africa project. Another compromise had to be made in those instances – operate the drone at times when the raptors were not flying.

Overall the operation of the Matrice 210 drone with accessories has been productive and successful.

4. IMAGE PROCESSING

The concept of cross-correlating multiple drone images into orthomosaics is well established and routine nowadays. Multiple companies sell commercial software or provide access to large computer clouds for the processing. Fast CPU’s and large working memory are essential. We typically process thousands of images in one single batch, where processing time can often be between 24-48 hours. Images are reviewed for any blurred imagery that can often occur when the drone rotates between flight lines. It can also happen sporadically in the thermal imagery as the thermal camera is more sensitive to turbulence than the optical camera. This work requires patience and concentration. When the drone images are fully uploaded to orthomosaic processing, the procedure generally runs without interruption until the entire batch of images has been processed.

Figure 2 demonstrates how multiple drone images support determination of a single pixel location in an initial sparse reconstruction using Pix4D. The drone images are draped over the sky. The single point location where all green lines converge on surface is located in many of the drone pictures as an automatic tie point. The map software algorithms use these to determine coordinates and as a basis for a dense point cloud, which is used to generate an orthomosaic and DSM in the final processing stages. With high accuracy coordinates such as ground control points and geothermal well coordinates, the coordinate precision can be improved to a centimeter-level offset. Our output maps generally have a horizontal offset of less than 2 meters without any ground control points while the elevation shift is generally larger.

The map precision can be improved within various commercial software bundles by optimizing the point cloud but the map outputs can also be corrected easily in GIS software like QGIS (QGIS Development Team, 2018) which is most handy in georeferencing orthomosaics to the actual well locations as well as countless methods of post-processing and analysis.

The resulting GIS themes can grow to be very large. Currently our largest is about 5.8 GB of a 9 km^2 aerial photo delivered as single file object. We find it essential to build a multi-layer pyramid structure into such themes for a faster zooming in and out in GIS software.

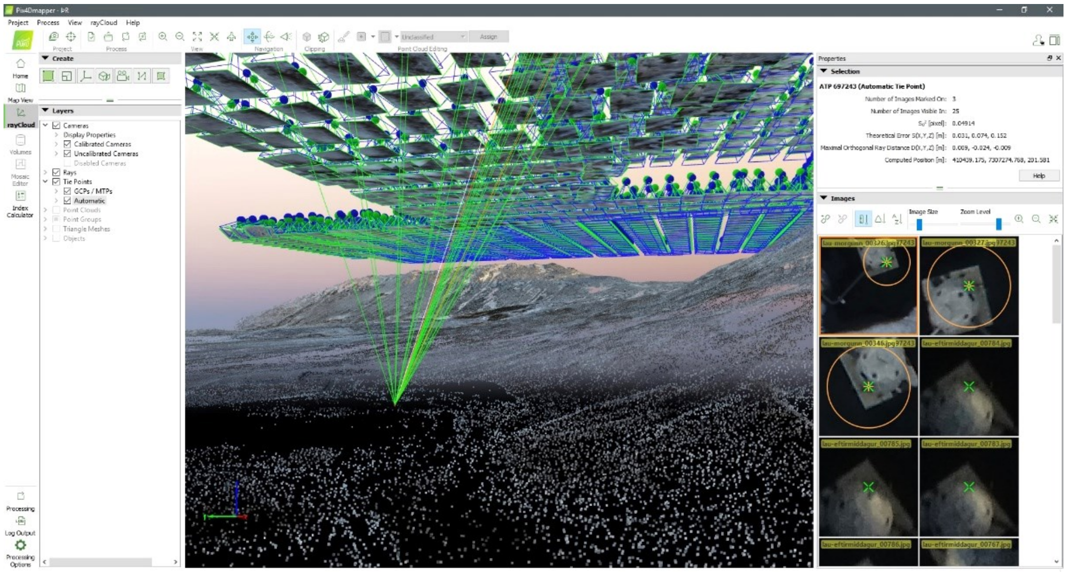

Figure 2: A 3-D perspective on how a single tie point is constructed using multiple drone images

The thermal map processing is a special story. The Zenmuse FLIR XT thermal camera delivers thermal imagery with the proprietary R-JPEG file format that contains raw thermal values internally along with a complex metadata section. At the time of purchasing the drone, commercial solutions for thermal mapping were fewer and less accessible. The authors therefore proceeded to write their own Linux and Python scripts to convert the proprietary R-JPEG files to a format more easily recognized by most commercial map processing software. By overcoming this hurdle, the thermal exploration mapping together with conventional drone mapping has in our opinion advanced to a commercial stage. For example, our two most recent projects mapped 10.5 and 16 km^2 in 3 and 8 days respectively. The area coverage is so high since the drone team has been able to improvise a solution where both drone cameras are shooting simultaneously.

Apart from the various features and technical parts of conducting thermal imaging with a drone, we have learned that detecting thermal anomalies and plotting appropriately is another learning curve to pass. Simple climatic issues like high air humidity are to be avoided as the thermal radiation signal is partly absorbed by the air humidity. Solar effects can then become significant and produce hot pixels which need to be separated from actual geothermal anomalies. Solar effects can also mask fainter geothermal anomalies. Night flying is best for mitigating solar influence at the cost of not sampling optical images during the same flights. Any drone operator therefore needs to weigh the pros and cons of flying at night or day, high or low and so forth.

Finally, we have observed that the Zenmuse XT's temperature readings are sensitive to the drone flying with or against cold wind, and within time of the day. The resulting thermal map, when plotted for the entire survey area of many km^2 may therefore look dominated by cooler and hotter stripes. Sub-arctic environments such as Iceland do not always offer ideal climatic conditions for thermal mapping, making drone flight missions during cold winds nearly inevitable. Such striping phenomenon is well known in geophysical mapping. It can be mitigated or even removed by filtering out longer wavelengths by appropriate software generally in the Fourier domain. Figure 3 shows as an example how such banding, that dominated an unfiltered temperature map in Þeistareykir, Iceland, has been removed by filtering out all wavelengths between 66 cm and 66 meters. The resulting filtered map looks dull but is misleading as impressive features in the thermal manifestation become visible when zooming in.

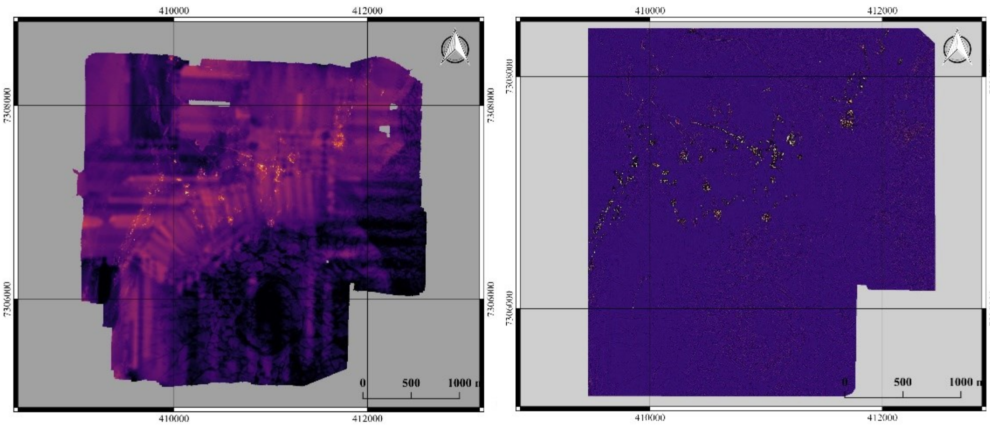

Figure 3: Unfiltered thermal map with stripes (left) being removed by FFT software (right)

5. THERMAL IMAGING IN SVARTSENGI, ICELAND

The eastern half of the Svartsengi reservoir was mapped for an aerial orthomosaic, DSM and thermal map in early June 2018. First flights took place on June 4 and the resulting orthomosaics maps with a report were delivered on June 26, 2018. The weather was not in our favor: drizzling rain with sunny spells in between. The short 40-minute drive from Reykjavík made up for aborting several flights when it was too humid. A weather station operated by the Icelandic Road and Coastal Administration proved most helpful in planning the field work and selecting temperature pixels of geothermal significance. It namely displayed both the air humidity and the black asphalt road temperature on a frequently updated webpage. Thermal camera flights could therefore be limited to 80% or less air humidity while the black road surface hardly exceeded 26 °C temperature during the day. The resulting map shown in Figure 4 emphasizes thermal map pixels that are hotter than 27 °C, now taken as of geothermal significance thanks to the road temperature data.

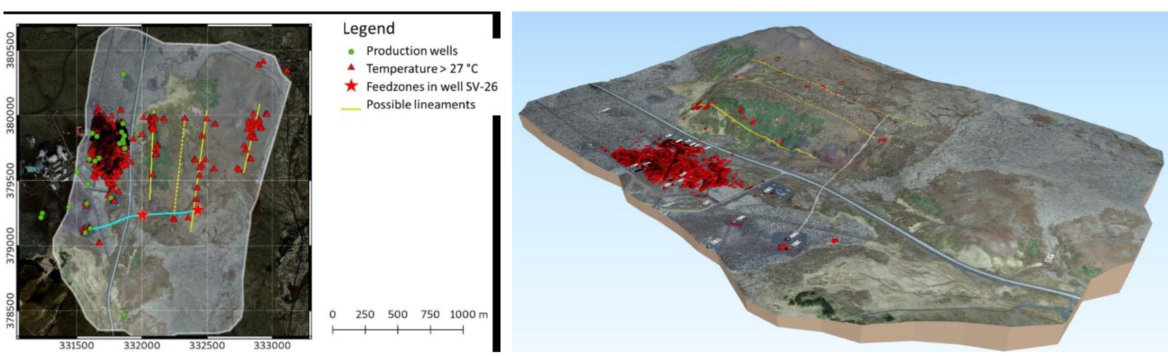

Figure 4: Temperature pixels (Δ) hotter than 27 °C and a 3-D perspective draped on the 3 km^2 aerial photo

The map in Figure 4 is showing the east margin of the current Svartsengi wellfield. Of significance are steaming grounds on the map west margin that relate to leaking caprock of the geothermal reservoir. Steam escape was actually amplified to the area after production dropped the reservoir pressure by 10-20 bars, explained by a pressure rise under the reservoir caprock when the pressure gradient jumped from that of boiling point with depth to vapor static (Bjornsson 1999). The low mountain to the east of the steam cap fumarolic area also shows signs of three N-S striking lineaments of warm grounds that are regarded as possible, permeable and near vertical structures. The trajectory of well SV-26 is shown on the map and red stars represent loss zones in the well. Apparently, there is a correlation between them and two of the suggested lineaments seen by the drone. It should be noted that these higher elevation anomalous temperatures are not known to emit steam to surface on cold winter days. If true, we find likely that the rising steam from depth is being condensed within the mountain while the CO_2 gases make it to surface slightly heated relative to the surroundings. Such a phenomenon of a non-thermal manifestation is known to the geothermal community, a suggested term is Kaipohan (Bogie et al., 1987).

6. THE GREAT GEYSIR FUMAROLE AREA IN S-ICELAND

When getting up to speed with the drone operations, mapping the Great Geysir fumarole area in S-Iceland was an obvious choice. Logistics were on the other hand a bit tricky as the area is a popular tourist destination which, like the thermal manifestations themselves, will make groups of people show up in the thermal map and distort readings. More importantly, drone regulations and common courtesy prohibits flying drones over large crowds. The field crew therefore decided to overnight in a local hotel and fly the drone in the very early morning hours of August 2nd 2018. The resulting 0.7 km^2 map is shown in Figure 5, collected in less than 2 hours. A flying height of 120 m over ground was selected for higher resolution of the thermal map. The spectrum of surface temperatures, from only about 6 °C that is typical for lowland groundwater reservoir up to around 90 °C in the Blesi boiling hot spring surface, are observed using an emissivity of 0.95. Such temperatures are convincing and infer the thermal maps are properly converted to near true surface temperatures.

Despite the Great Geysir area being very well known, recent scientific studies on the reservoir are scarce. See Pasvanoglu et al. (2000) for an overview. The area is interesting for seeing both the geothermal water and the steam emit to surface, bringing to life the famous Geysir and Strokkur eruptive springs. The field is at the south margin of rhyolitic intrusives believed to work as a heat source while N-S oriented seismically active faults that relate to the S-Iceland transverse seismic zone provide the vertical permeability. This line of permeability shows up clearly in the thermal map in Figure 5. Many other features of interest are to be seen. For example, hiking trails are warmer than the nearby areas, here interpreted as compaction that either hinders evaporative heat loss to the ambient or increases the heat conductivity of the top soil.

The water bowls of the Great Geysir and Strokkur each host lively convection cells that are shown in the two inserts on Figure 5. Geysir is dormant now while Strokkur is very much active and erupts regularly several times per hour. Inspection of their surface temperature shows quite a variation, like some 7 °C in Geysir. Note also in the figure's lower center part a straight-line thermal anomaly striking to the ESE. This is a hot water pipe to nearby hotels and houses that is poorly or not insulated.

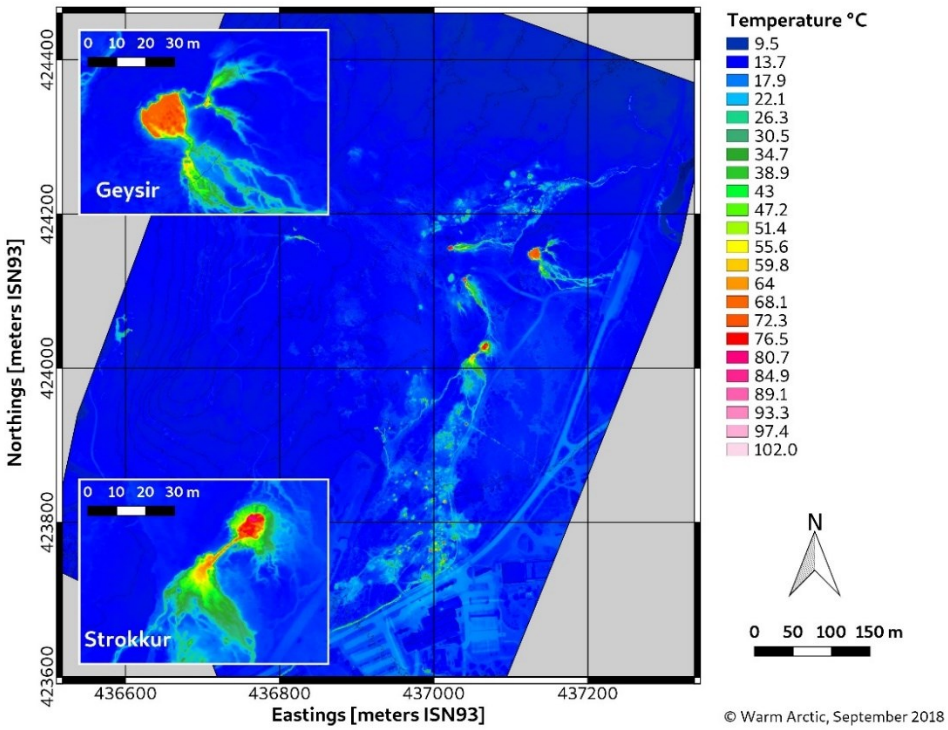

Figure 5: Surface temperature map of the Great Geysir area in S-Iceland

7. HEAT EMITTED FROM THE 1973 ELDFELL VOLCANCI CRATER IN HEIMAEY, S-ICELAND

The 5000-inhabitant fishing town of Heimaey in S-Iceland made world news headlines when struck by a volcanic eruption only some 800 m from the town center in January 1973. The eruption quickly became confined to a single vent that was later assigned the name Eldfell. Some 80 m of basaltic lava piled up around the crater and posed a threat to the community but was later diverted by massive lava cooling operations (USGS, 1997). When the eruption ceased, the township of Vestmannaeyjar slowly rebuilt and continued to flourish as an important fishing village. Less known however is a successful 10 years of district heating operation that was sustained by spraying water on the solidifying lava pile and capturing the rising steam. Various mathematical models were made on the lava solidification process and used to support the decision to build a district heating system for the town (Bjornsson, 1980; Bjornsson et al, 2020).

We decided to map the temperature of the Eldfell summit on a sunny and windy day in late August 2018. Figure 6 shows the results. The dark colored crater surface and sunny weather made us only show temperatures in excess of 30 °C on the map. Striping is seen in the temperatures that correlate with the drone flying with and against a strong northerly wind. Despite these solar-originated thermal contaminants, the image clearly shows around 70 °C steam rising from the crater's SE summit rim. Furthermore, hot spots are seen in the lava field to the east of the crater where the deposited lava field is estimated as thickest. This simple survey lasting some 12 hours door to door for the field work infers that even today, some 45 years after eruption, the Eldfell lava pile is still to fully cool down. Thermal mapping with drones therefore appears as suitable tool for volcano monitoring.

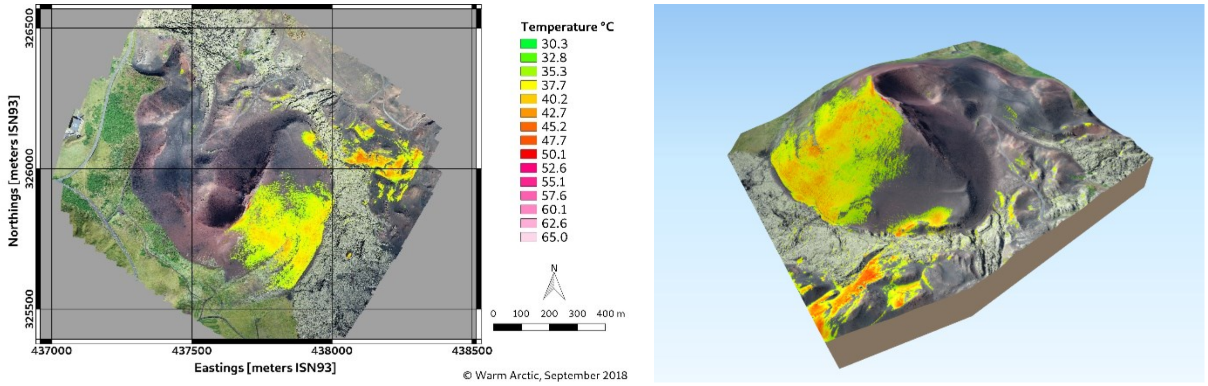

Figure 6: Surface temperature map of Eldfell (left) and in a 3-D perspective (right)

8. THE SNÆFELLSJÖKULL VOLCANO FLANK

Driven by curiosity the Warm Arctic drone team decided to map a volcanic crater to the east of Snæfellsjökull, a dormant stratovolcano in W-Iceland, where a manned weather station operated on the crater rim back in 1932-1933. At some 830 m elevation above sea-level, conditions were harsh and offered limited opportunities for outdoor activities. The weathermen, however, had the opportunity to explore their surroundings to make this observation: *"At -15 °C outdoor temperature we entered a cavity under the winter snow to measure +9 °C temperature."* These measurements are considered reliable as the operation was meteorological. The same spot stayed green in the summer (www.timarit.is, in Icelandic).

Although considered dormant, the Snæfellsjökull volcano has a lively history and appearance (Sigurðsson, 2017) and should not be neglected for its volcanic hazard and possibly hosting a high temperature geothermal resource. The Warm Arctic team mapped this area with a drone in conjunction with an end of summer staff celebration. The weather was sunny and warm, making the interpretation of the temperature map less straight forward. Figure 7 shows in a 3-D perspective the old weather station crater area where the mid-winter 9 °C temperature was measured back in 1932-1933. Several features in the map are indicative of geothermal gases rising to surface in the area. For example, relatively thick moss vegetation was observed on the north side of the crater at 830 m elevation. Surrounding mountain peaks did not appear to have comparable amount of vegetation, although some ridges had a faint greenish hue that may resemble another species of moss. Secondly there are melting forms in the winter snow. One such is shown with an arrow on the right-hand side of Figure 7 and more are seen in the 1 km^2 being mapped. The cavity soil layer was dug out by some 10 cm to find 9 °C temperature under the frozen surface.

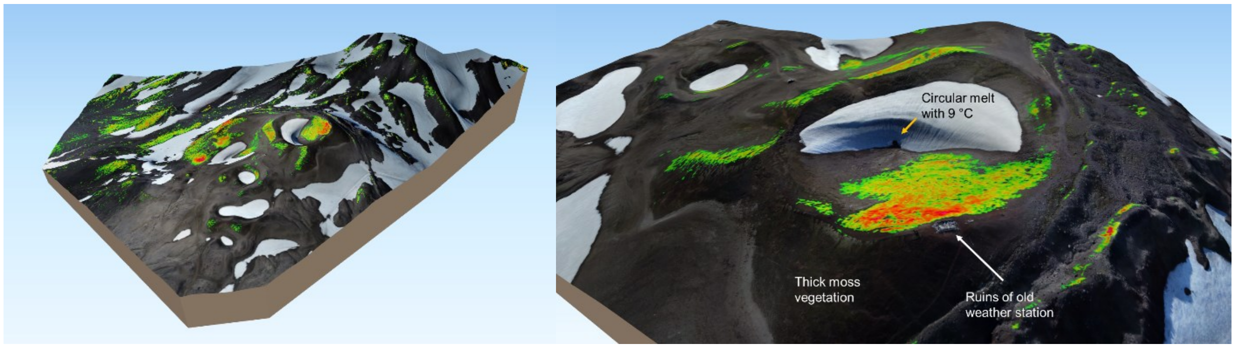

Figure 7: 3-D perspective of the crater rim hosting the 1932-1933 weather station. View to the SW.

The Snæfellsjökull mapping exercise is rather inferring than proving the existence of a possible boiling geothermal reservoir buried deep into the strata. Continuous flux of steam and gas to the surface can however explain many of the features seen. Like in the case of Heimaey, both sites should be mapped overnight for less solar effects. CO_2 soil gas flux meters would also be interesting and these can operate on snow for better contact with the ground.

9. WAY FORWARD

Our experience operating a drone carrying both thermal and optical cameras has been fruitful and interesting. With experience and sufficient number of batteries it also should become fast and cost effective, thereby becoming a standard field data set in geothermal development and operations.

With his 30 years of geothermal work worldwide, the first author of this paper is approaching the drone thermal maps a bit differently than in some of the earlier research. First of all, the drone equipment should be as much automated and precise as possible to allow the user to focus on the collected data, not the equipment. Secondly the shape and location of temperature anomalies is as important as using the thermal maps for estimating heat losses to the ambient. With millions of pixels collected the geothermal anomaly picking looks to be one of the challenging future works needed. The geothermal anomalies, despite being very weak, namely infer locations of vertically permeable structures. When lining up on a map, these add confidence to well prognosis and ideally average well success. Such field data set will in turn move from nice to needed.

Environmental monitoring is another field of interest where thermal mapping should contribute. Here some simple statistical analysis can assist like counting the temperature pixels within a certain temperature range. When multiplied with the pixel size, histograms can be made with hectares of ground within each range. Repeated surveys will then show if the geothermal development is affecting the surface expression of the resource.

Finally, artificial intelligence may assist in the large thermal map interpretation. In this present study, lineaments of geothermal importance are found quickly by ignoring all temperatures below a certain threshold. Although this method is effective, it excludes lineaments that are perhaps characterized not by high temperature, but by more complex patterns or features. These can be found by examining the orthomosaics with the naked eye. However, this is a tedious and time-consuming approach which furthermore requires expertise in the field. Since Warm Arctic has collected vast amounts of thermal and optical images of geothermal areas, a possible method to detect these lineaments automatically could lie in a data-driven approach. Advancements in the field of machine learning and deep learning (LeCun et al. 2015) have made it easy to classify large image datasets by using convolutional neural networks. By manually labelling and distinguishing individual thermal images that contain complex lineaments or not, it is possible to train a neural network to classify new images on whether they contain a lineament or not. This trained neural network could then be used to automatically highlight new images that might contain interesting lineaments, which could then be inspected more closely by experts.

Another approach might be to train an autoencoder (Le, 2013) to reduce the dimensionality of the image sufficiently. The reduced image could then be used to train a one class support vector machine, or OSVM (Weston & Watkins, 1998). An advantage of this method is that an OSVM can be trained only on ‘normal’ images without lineaments, and if it sees an image that is an ‘anomaly’ compared to the normal images, it will flag them. This report attempted a crude and quick implementation of this method on images obtained in a recent Africa project, which showed promising results. After quickly training an OSVM model on images that did not contain any lineaments, it was already able to report anomalies in images that it had not yet seen with significantly higher-than-chance precision. With more work and training, it is likely very feasible to obtain a more reliable and precise model.

Finally, the drone detection of CO_2 non-thermal anomalies looks promising and adds a new dimension to the exploration work. Here lies an opportunity in detecting periphery or high elevation geothermal discharge locations with faint to none temperature anomalies. For example, the Þeistareykir mountain manifestations are of only about 2-4 °C higher temperature than the surrounding grounds and would have been missed if not for melting the ground snow layer. Several authors like Harwey et al. (2018) have already begun work on this important geothermal outflow property but use a ground flux gas meter operated on foot. CO_2 electronic and atmospheric gas meters are available on the market and ideally these also have a wave spectrum to be picked up with the right multispectral camera mounted to a drone.

10. CONCLUSIONS

Integrated drone systems of thermal and optical cameras have proven to be a fast, reliable and cost-effective solution in mapping surface features of geothermal reservoirs. The road from beginning to profession will however take time and learning. A large volume of field information is collected and we envisage that artificial intelligence will play a role in fully utilizing this data set. Support to reservoir structural models is deemed as or more important than heat loss estimates.

REFERENCES

Abubakar A. J., M. Hashim, A. B. Pour and K. Shehu: A Review of Geothermal Mapping Techniques Using Remotely Sensed Data. Science World Journal Vol 12 (4), ISSN 1597-6343 (2017)

Björnsson S.: Natural Heat Saves Millions of Barrels of Oil: Unique Procedures Developed by Icelanders—They Even Tap Hot Lava. Atlantica and Iceland Review, v. 18, no. 1, p. 28–37 (1980)

Bjornsson G.: Predicting Future Performance of a Shallow Steam-Zone in The Svartsengi Geothermal Field, Iceland. Proceedings, Twenty-Fourth Workshop on Geothermal Reservoir Engineering Stanford University, California (1999)

Björnsson S., B. Jónasson and M. Karlsson: Heat of Molten Lava Used for Space Heating. Proceedings World Geothermal Congress, in press (2020)

Bogie I., J. V. Lawless, J. B. Pornuevo: Kaipohan. An apparently nonthermal manifestation of hydrothermal systems in the Philippines. Journal of Volcanology and Geothermal Research. Volume 31 (3–4) pp 281-292 (1987)

Cherkasov S.V, A. M. Farkhutdinov, D. P. Rykovanov and Arbi A. Shaipov: The Use of Unmanned Aerial Vehicle for Geothermal Exploitation Monitoring: Khankala Field Example. Journal of Sustainable Development of Energy, Water and Environment Systems, Vol. 6 (2) pp 351-362 (2018)

González L. M. R.: Remote sensing of surface hydrothermal alteration, identification of minerals and thermal anomalies at Sveifluháls-Krýsuvík high-temperature geothermal field, SW Iceland. Master’s thesis, Faculty of Earth Sciences, University of Iceland (2018)

Harvey, M.C., S. Pearson, K. B. Alexander, J. Rowland and P. White: Unmanned aerial vehicles (UAV) for cost effective aerial orthophotos and digital surface models (DSMs). Proceedings New Zealand Geothermal Workshop (2014).

Harvey M. C. and K. M. Luketina: Thermal Infrared Cameras and Drones: A Match Made in Heaven for Cost-Effective Geothermal Exploration, Monitoring and Development. 37th New Zealand Geothermal Workshop (2015)

Harvey M., C. Harvey, J. Rowland and K. Luketina: Drones in Geothermal Exploration: Thermal Infrared Imagery, Aerial Photos and Digital Elevation Models, Proceedings, 6th African Rift Geothermal Conference. Addis Ababa, Ethiopia (2016a).

Harvey, M. C., J. V. Rowland, and K. M. Luketina: Drone with thermal infrared camera provides high resolution georeferenced imagery of the Waikite geothermal area, New Zealand. Journal of Volcanology and Geothermal Research (2016b)

Harvey M., G. Chavez and M. Delgado: CO_2 Flux Surveys for Geothermal Exploration in Arid Environments. 43rd *Workshop* on Geothermal Reservoir Engineering. Stanford, California (2018)

LeCun, Y., Bengio, Y., and Hinton, G. Deep learning. Nature, 521 (2015).

Le, Q. V.: Building High-Level Features Using Large Scale Unsupervised Learning. In Acoustics, Speech and Signal Processing (ICASSP), 2013 IEEE International Conference (2013).

Ólafsson J. M.: UAV Geothermal Mapping in Austurengjar. Master’s thesis in Sustainable Energy. Reykjavik University (2018)

Pasvanoglu S., H. Kristmannsdóttir, S. Björnsson and H Torfason: Geochemical Study of The Geysir Geothermal Field in Haukadalur, S-Iceland. Proceedings World Geothermal Congress (2000)

QGIS Development Team. QGIS Geographic Information System. Open Source Geospatial Project. http://qgis.osgeo.org (2018)

Sigurðsson H.: Snæfellsjökull, Art, Science, History. Book. Publisher Stykkishólmur Vulkan (2017)

USGS: Lava-Cooling Operations During the 1973 Eruption of Eldfell Volcano, Heimaey, Vestmannaeyjar, Iceland. U.S. Geological Survey Open-File Report 97-724. Editor Richard S. William, Jr. (1997)

Vaughan R. G., D. Bergfeld, W. C. Evans, S. Wilkinson, C. Miwa and M. Diabat: A Baseline Thermal Infrared Survey of Ground Heating Around the Casa Diablo Geothermal Plant, Mammoth Lakes, CA. Geothermal Resources Council Transactions (2018)

Weston, J., & Watkins, C.: Multi-Class Support Vector Machines. Technical Report CSD-TR-98-04, Department of Computer Science, Royal Holloway, University of London (1998)